DTU Library

Active vibration-based SHM system: demonstration on an operating Vestas V27 wind turbine

Tcherniak, Dmitri; Mølgaard, Lasse Lohilahti

Link back to DTU Orbit

Active Vibration-based SHM System: Demonstration on an Operating Vestas V27 Wind Turbine

Dmitri TCHERNIAK [1], Lasse L. MØLGAARD [2]

[1] Bruel & Kjær Sound & Vibration,
Skodsborgvej 307, Nærum 2850, DENMARK, dtcherniak@bksv.com
[2] Dept. of Applied Mathematics and Computer Science, Technical University of Denmark,
Kgs.Lyngby 2800, DENMARK, llmo@dtu.dk

Key words: wind turbines, blade damage, actuator, accelerometers.

Abstract

This study presents a system that is able to detect defects like cracks, leading/trailing edge opening or delamination of at least 15 cm size, remotely, without stopping the wind turbine. The system is vibration-based: mechanical energy is artificially introduced by means of an electromechanical actuator, whose plunger periodically hits the blade. The induced vibrations propagate along the blade and are picked up by an array of accelerometers. The vibrations in mid-range frequencies are utilized: this range is above the frequencies excited by blade-wind interaction, ensuring a good signal-to-noise ratio. At the same time, the corresponding wavelength is short enough to deliver required damage detection resolution and long enough to be able to propagate the entire blade length.

The paper demonstrates the system on a 225 kW Vestas V27 wind turbine. One blade of the wind turbine was equipped with the system and a 3.5 month monitoring campaign was conducted while the turbine was operating normally. During the campaign, a defect – a trailing edge opening – was artificially introduced into the blade and its size was gradually increased from the original 15 cm to 45 cm.

Using an unsupervised learning algorithm, we were able to detect even the smallest amount of damage while the wind turbine was operating under different weather conditions. The paper provides the detailed information about the instrumentation and the measurement campaign and explains the damage detection algorithm.

1 INTRODUCTION

Blades of modern wind turbines are designed for 20–25 year service under severe weather conditions, and during this period damage is unavoidable. With a high probability, a small blade defect may develop into a bigger failure, and if no countermeasures are taken, may become critical, causing catastrophic consequences. Repair of a small defect is significantly cheaper than repair of a bigger one or entire blade replacement. Therefore, wind turbine operator companies pay close attention to structural health monitoring of the blades. Today this is done by periodical visual inspections conducted every one-to-two years but many in the industry realize that a better approach is needed. The suggested approaches attack the problem from very different directions [1]; alongside using more robust blade design and special surface treatments to protect the blades, they include, for example, facilitating visual monitoring by

means of transportable ground-based optical systems, by drones equipped with high-resolution video cameras, using thermography and many others techniques.

One of the most promising ways is instrumenting wind turbines with vibration sensors and monitoring the blades' integrity via permanent monitoring of their vibration, [2], [3]. This approach is already adopted for monitoring the mechanical components of wind turbines, such as gearbox and bearings. The main advantage of such a system is that the operator/owner is notified about the occurrence of damage almost immediately after it has happened and not after one-two years, when it is detected by visual inspection.

Structural health monitoring via vibration monitoring may be based on different physical phenomena. One of the popular vibration-based approaches is detecting changes in modal parameters: loss of structural integrity leads to stiffness reduction, which can be detected by monitoring modal parameters. However, this approach cannot achieve the required damage resolution since the modal parameters are not very sensitive to damage [4]. Another well-known vibration approach is based on guided waves [5]: a piezoelectric exciter generates stress waves, which propagate through the structure and get picked by another piezoelectric sensor. Typically, a network of active sensors (which can measure and generate vibrations) is used. Blade damage can be detected and localized by monitoring how the vibration propagates from the actuators to the sensors. The guided waves approach has much better damage resolution but requires high sensor density, since the high-frequency oscillations quickly decay with the propagation distance. Using a large number of sensors adds complexity to the SHM system and negatively influences its cost, making it less attractive for the end users.

In study [6], the authors introduced another technique (patent pending), which is similar to the guided waves technique but has inherent differences: the excitation is introduced by an electromechanical actuator, and the utilized frequency range is much lower compared to the guided waves approach. The introduced vibrations are picked by an array of accelerometers. The waves at the lower frequency (around 1 kHz) can propagate longer distances, thus the technique requires far fewer sensors. At the same time, the frequency is high enough to ensure sufficient damage detection resolution (at least 15 cm size). Structural damage changes the properties of the energy propagation between the actuator and the accelerometers; this can be detected comparing the vibration pattern in a reference (healthy) state with the damaged state.

The important feature of the suggested approach is that it is possible not only to detect damage but also to follow its development, [6]. Additionally, studies [7], [8], [9] demonstrated the possibility to use the technique for damage localization.

In [6] the method was applied to an SSP34m blade (34 m long), mounted on a test rig. The presented study reports the results when the same technique was used on an operating wind turbine.

2 SYSTEM IMPLEMENTATION ON VESTAS V27 WIND TURBINE

Study [6] describes the experiment conducted on an SSP34m blade mounted in a test rig. Test rig facilities greatly simplified the experiment: since the blade did not move and was located indoors, much less care had to be taken about mounting of accelerometers, actuators and cabling. The experiment proved that the proposed approach performs well on a modern blade, with feasible actuator location and using a reasonable number of sensors. It managed to detect a realistic blade fault (trailing edge opening) and follow up on its progression. However, using the test rig, we could not evaluate how robust the method was against noise. Indeed, when operating, the wind turbine blade is subjected to wind excitation and excitation from the hub and nacelle mechanisms, which mask the signal from the actuator. In [6] some artificial

noise (recorded on the blades of another wind turbine in operation) was mixed with the measured signals from the actuator: we had to admit that the selected signal-to-noise ratio was very much a guess. In addition, to be able to show the technical feasibility of the proposed system, it was important to demonstrate it on an operating wind turbine.

Vestas V27 wind turbine was selected for the experiment due to its availability. The wind turbine stands on the grounds of Technical University of Denmark (DTU), Department of Wind Energy (formerly known as Risø), in Denmark, near town of Roskilde. Vestas V27 is a relatively old wind turbine, with 27 m rotor diameter and 225 kW rated power. However, this wind turbine can be considered representative of many modern wind turbines: it is an upwind, pitch regulated, horizontal axis wind turbine. In contrast to modern wind turbines, its blades are relatively stiff, and it has only two speed regimes: 32 and 43 rpm.

For blade excitation, the same actuator was used as for the SSP34m blade experiment (Figure 1a). The actuator is a simple electromechanical device: a coil is mounted on a steel base; driven by an electrical pulse, the coil "shoots" the plunger towards the structure; after the hit, the plunger returns to the initial position by means of a spring.

Due to the size of the blade, it was not possible to install the actuator inside the blade (as was done on the SSP34m blade). Instead, the actuator was installed outside the blade, on its upwind side about 1 metre from the root, covered by a waterproof lid and secured with a strap (Figure 1b,c).
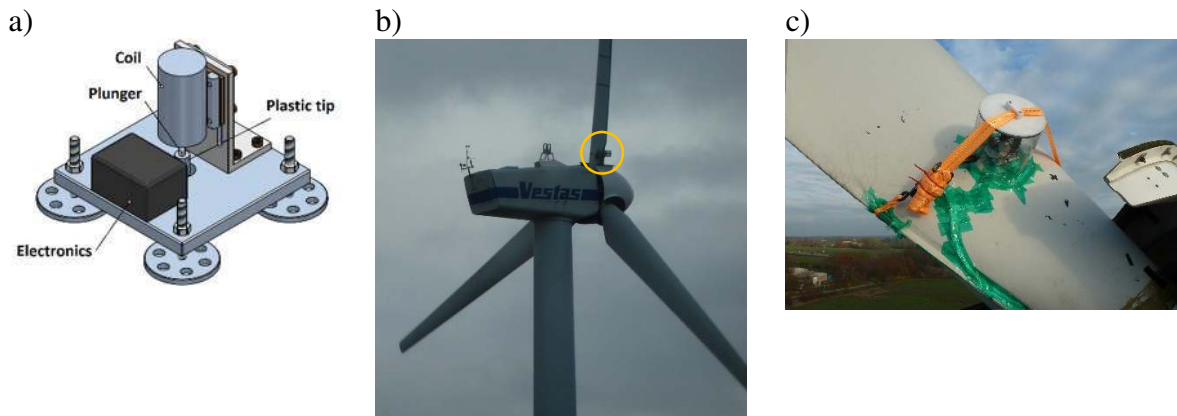

Figure 1. Actuator: a) design; b) actuator location, inside the circle; c) installation on the blade.

The vibrations were measured by accelerometers. The blade was instrumented with twelve monoaxial piezoelectric accelerometers (Brüel & Kjær Type 4507B); their location is shown in Figure 2a. The nominal sensitivity of accelerometers #5 - #15 was 10 mV/ms^{-2} (Type 4507-B-004) and accelerometer #16, located near the actuator, had nominal sensitivity 1 mV/ms^{-2} (Type 4507-B-001). For mounting the accelerometers, we used plastic mounting clips, which were glued directly to the blade (no special alignment was performed, the accelerometers' measurement direction was normal to the blade surface). To protect the accelerometers, they were covered by silicon, then "helicopter tape" was applied on top to give the silicon a smooth shape (Figure 2b). The accelerometers and cables were placed on downwind side of the blade.

The accelerometer cables run from the accelerometers towards the trailing edge and then along the trailing edge towards the blade root (Figure 2c). The cables were glued to the blade with silicon and covered with helicopter tape. Experience from the previous long measurement campaign on the same wind turbine [10] was used. From the same experience, we knew that

3

such an arrangement could last several months, which is sufficient for the planned campaign, but obviously not good enough to survive on the blade for several years. For the latter case, other arrangements must be developed.
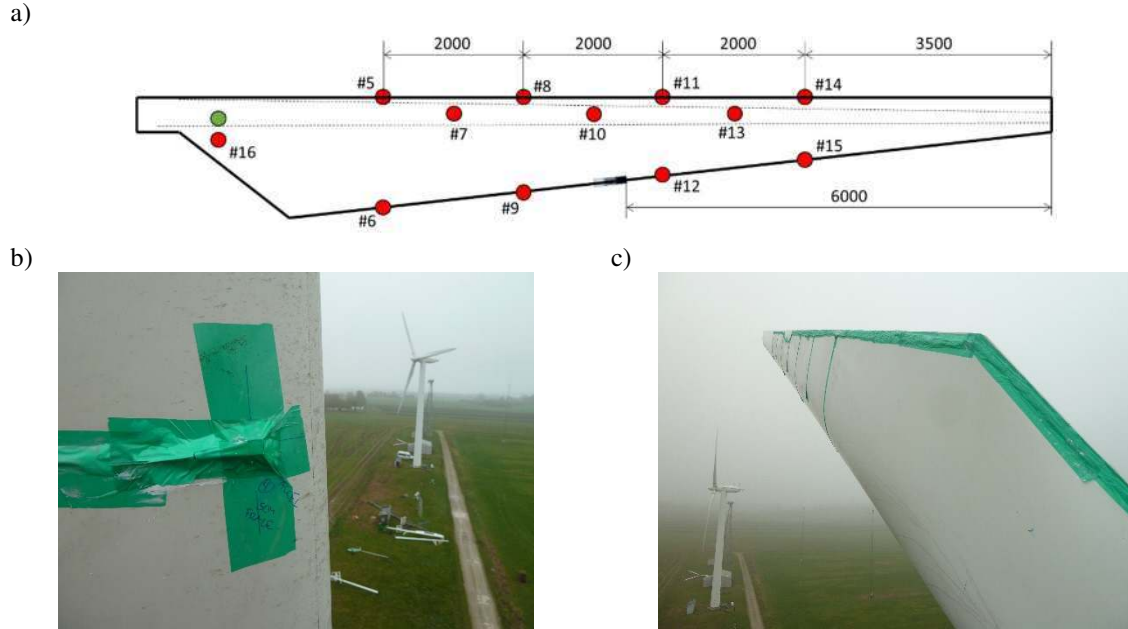
a)

b)

c)

Figure 2. Blade instrumentation: a) red circles – location of the accelerometers; green circle – actuator location; b) accelerometer mounted on the blade; c) cable arrangement.

The accelerometers were connected to a data acquisition system (Brüel & Kjær Type 3660-C with two LAN-XI modules, a 12-channel input module Type 3053-B-120 and 4-channel input/output module Type 3160-A-042). Two piezoresistive DC accelerometers Type 4574-D mounted in the spinner were used to estimate the rotor azimuth with a possibility to derive the rotational speed of the rotor. In addition, the pitch angle was measured.

The actuator was controlled by the signal from the signal generator built into one of the data acquisition modules. The generated rectangular pulse triggered the actuator's electronics, making a 100 μF capacitor discharge through the coil. Then the capacitor was charged again to 48 V using a DC/DC converter to be ready for the next shot.

The data acquisition system and the electronics were placed in a waterproof box (dimensions $60 \times 45 \times 20$ cm^3 and weight 25 kg), which was mounted to the inner surface of the spinner (Figure 3). The equipment was powered by 24 V from the nacelle via a slip ring.

The measured data (in total 16 signals sampled with 16384 Hz frequency) was wirelessly transmitted from the rotating part to the nacelle via two Cisco wireless access points, one located inside the waterproof box and another installed in the nacelle. When the turbine is operating, the line of sight between the hub and nacelle might be blocked by the steel parts of the hub. To keep an uninterrupted wireless connection, two pairs of antennas were employed: two omnidirectional antennas attached to the hub and two directional antennas mounted inside the nacelle.

The data acquisition system was controlled by Brüel & Kjær PULSE LabShop software. The software was programmed to start data acquisition, wait 10 seconds, initiate an actuator hit and measure for another 20 seconds. Then acquisition was stopped and the system waited

4

for four and a half minutes and initiated again. Thus, 12 actuator hits and corresponding datasets were produced every hour. Typical signals are shown in Figure 4.
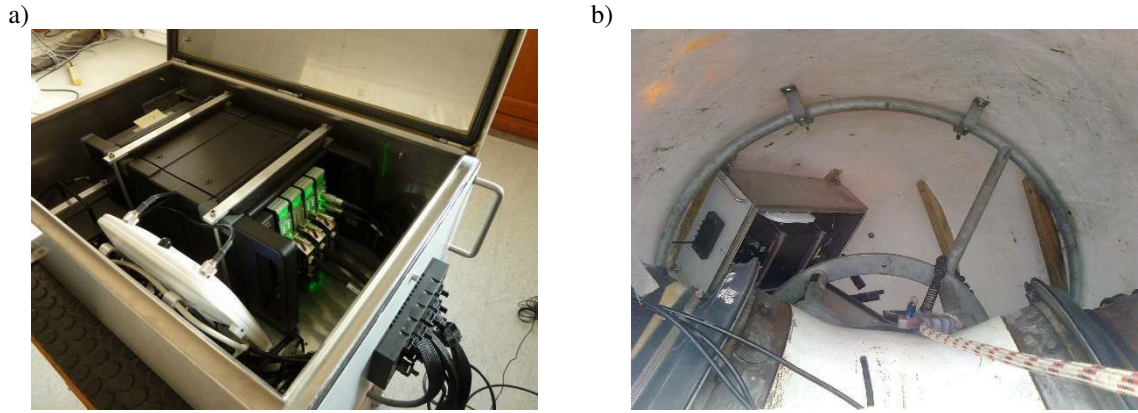
a)

b)

Figure 3. Data acquisition system: a) The waterproof box with LAN-Xi system (more modules are shown); b) the waterproof box is mounted inside the spinner but the cables are not yet connected.
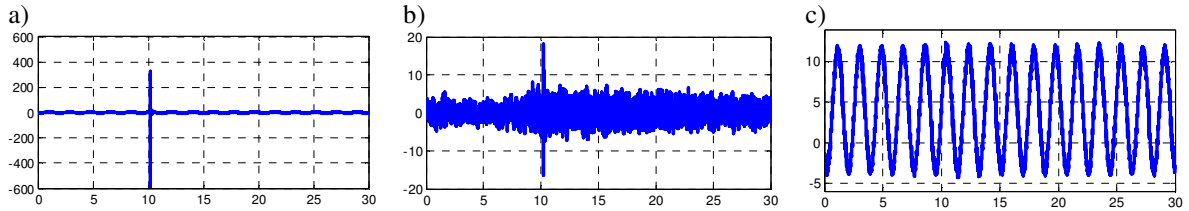

Figure 4. Typical signals: a) accelerometer #16 (20cm from the actuator); b) accelerometer #15 (8.5m from the actuator); c) DC accelerometer.

Simultaneously with the vibration data, meteorological data were collected from a nearby weather mast. The weather data included temperature, wind speed and direction, wind turbulence at different altitudes, atmospheric pressure, precipitation, etc.; the data from the mast were delivered averaged within one-minute intervals. The power production data and yaw angle (the angle between the wind and orientation of the nacelle) was also available from the wind turbine system.

3 EXPERIMENT

The measurement campaign was started Nov. 28, 2014 and finished Mar. 12, 2015, thus lasting 104 days. With 12 actuator hits per hour (6 hits per hour during the Christmas and New year eve period), data from 24693 actuator hits were collected. During this time, the wind turbine was subjected to different weather conditions. The monitoring period covers about 1/3 of a year, thus no season-related events were observed. During the campaign, the turbine was in normal power production regime, governed by its controller. However, following the agreement with the wind turbine owner, in the damaged state, we could only operate the turbine under visual surveillance, i.e., during working hours. For nights, weekends and holidays, the wind turbine was set to idling (no power production), though the SHM system was kept working.

5

4 DAMAGE IMPLEMENTATION

For validating the capabilities of the proposed SHM system, an artificial defect was introduced in the instrumented blade. The following considerations were taken into account:

(i) Input from wind turbine manufactures and service companies regarding blades' typical defects and their location;

(ii) Reparability of the defect: it should be possible to repair the blade inexpensively after the end of the experiment;

(iii) Risk of the artificial damage developing to critical should be minimal.

In addition to this, we planned to test another property of the proposed SHM system: the indication of damage progression. For this reason, we planned gradually increasing the size of the defect.

Taken the abovementioned into account, the trailing edge opening type of damage was selected. This is a typical defect for the blades manufactured using this technology; it is easy to introduce, extend and repair, and, according to experience, the probability that it can progress uncontrollably is very low.

The initial artificial damage was introduced Dec. 9, 2014 (Figure 5a) by technicians from service company Total Wind Group. The trailing edge was opened and extended to simulate a crack. The length of the opening was 15 cm. The opening was covered by helicopter tape to prevent atmospheric water from coming into contact with unprotected inner blade material. Dec.15, 2014 the opening length was extended to 30 cm (Figure 5b) and Jan. 06, 2015 to 45 cm (Figure 5c). Jan. 19, 2015 the defect was repaired. The defect location in the blade is shown in Figure 2a and zoomed in in Figure 5d.
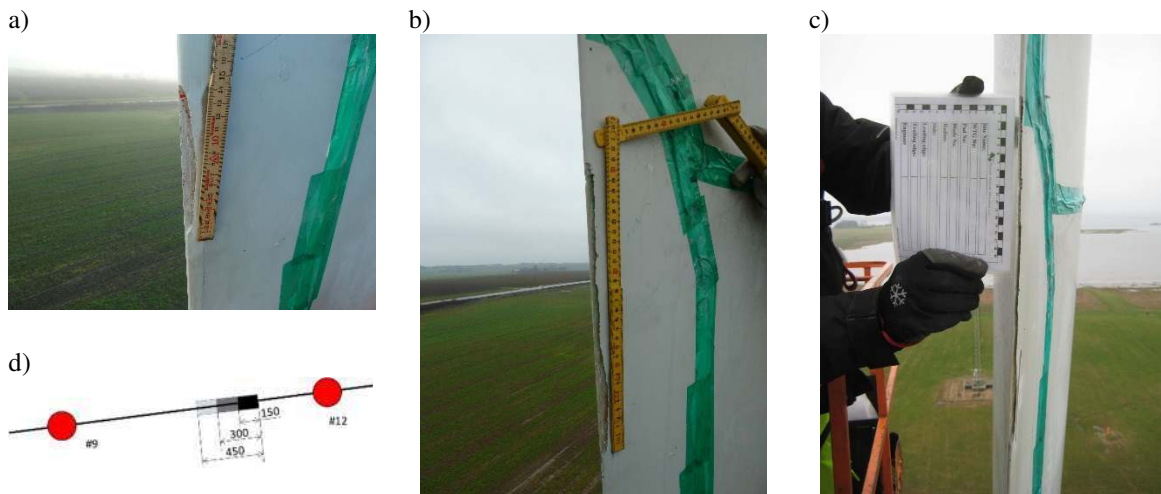

Figure 5. Implementation of the artificial blade damage. a) Initial 15 cm trailing edge opening; b) extended to 30 cm; c) extended to 45 cm. d) damage location in the blade relative to accelerometers, and its development: 15 cm > 30 cm > 45 cm correspond to black > dark grey > light grey.

5 DATA PROCESSING AND DAMAGE DETECTION

5.1 Classification

Damage detection can be seen from the classification perspective, and then vast knowledge accumulated in this area can be utilized for solving the SHM problems. Using the classification terminology, *semi-supervised anomaly detection* is the term describing our problem. Here we

assume that only the normal (healthy) state is known, and any deviations from this state are associated with damage. The damage detection procedure therefore includes two phases: the *training phase* and *detection phase*. During the first phase, we assume that the structure is undamaged; here, we collect a number of samples, characterizing the normal state under different operating regimes and establish a statistical model (or models, one for every wind turbine regime) of the normal state. During the detection state, every newly acquired sample is compared with the model of the normal state. If a significant deviation detected, we declare that the blade is damaged.

Calculation of each sample consists of two main steps: pre-processing and calculation of the feature vector, the steps are considered in the following sections.

5.2 Preprocessing

The data analysis started with processing the two DC accelerometers' signals to extract rotor rpm information and the rotor azimuth at the moment the actuator hit. Then the data from the accelerometers, pitch angle, extracted rotor rpm and rotor azimuth information were combined with the weather data and saved into a database to facilitate data access. The three main operating regimes were identified: idling, operating at 32 rpm and operating at 43 rpm. It was recognized that the vibrational data from the regimes cannot be compared directly, and further analysis was conducted separately for each regime.

Further pre-processing steps included:
1. Trimming the part of the signal around the actuator hit. This was done by detecting the beginning of the peak in the actuator control signal;
2. Fine alignment of the signals from different hits. This was done using the signal from accelerometer #16, closest to the actuator, since it is least affected by the noise;
3. Band-pass filtering. As mentioned in the introduction, a medium frequency range (around 1 kHz) is used. The band-pass filter was designed around this frequency (700–1200 Hz).

5.3 Feature vector

Following [11], elements of the covariance matrix were selected as a feature vector, characterizing the current blade's state. An acquired defect in the structure will change the energy propagation from the actuator to the sensors, which will affect the vibration pattern (relative magnitude and phase) of the measured acceleration signals. Since the covariance function is a measure of similarity between two signals, the changes in the vibration pattern will be reflected as a change in the cross-covariance matrix.

The covariance matrix is an $N \times N$ symmetric matrix, where N is the number of sensors selected for the analysis (either the full set or a subset of the sensors in Figure 2a). The number of distinct elements in the matrix is $K = N(N + 1)/2$. If all 12 sensors are selected, the size of the vector is 78, which may reduce the reliability of the statistical model. To avoid this, a dimensionality reduction based on principal component analysis is employed to find a representation with a smaller dimensionality K. The feature vector $\mathbf{y}_i \in R^K$, computed for i-th actuator hit, becomes a "sample", describing the state of the blade at time t_i.

5.4 Normal state and damage index

Assuming that the system is in undamaged state, let us measure M samples and build the matrix $\mathbf{X} = [\mathbf{x}_1, \mathbf{x}_2 \dots \mathbf{x}_M]$, $\mathbf{X} \in R^{K,M}$ The statistical properties of the matrix, its mean $\boldsymbol{\mu}_\mathbf{X} \in R^K$ and covariance $\boldsymbol{\Sigma}_\mathbf{X} \in R^{K,K}$ are considered as a simple statistical model of the normal state. The

7

Mahalanobis distance between a sample **y** and the state **X**:

$$d(\mathbf{y}, \mathbf{X}) = \sqrt{(\mathbf{y} - \boldsymbol{\mu_X})^T \boldsymbol{\Sigma_X}^{-1} (\mathbf{y} - \boldsymbol{\mu_X})}, \tag{1}$$

is a convenient metric to quantify the difference between the new sample and the normal state, which can play a role of the *damage index*. If the damage index is relatively small and does not exceed some threshold D, we conclude that the system is in undamaged state. Oppositely, if $d(\mathbf{y}, \mathbf{X}) > D$, we declare state **y** as damaged.

Following the unsupervised strategy, we should base the choice of the threshold D exclusively on the observations from the training phase. The assumption that all points in the training set are normal yields

$$D = \max_i (d(\mathbf{x}_i, \mathbf{X})), \tag{2}$$

but this choice is sensitive to outliers that might happen in the training set. To avoid this, we assume that the covariance data is normally distributed. Consequently, the Mahalanobis distance squared (d^2) follows a χ^2-distribution with K degrees of freedom. The value of the threshold, D, can then be obtained as, for example, the 99th percentile of the χ^2_K-distribution, which means that only 1% percent of normal data would exceed this value. This will provide a more conservative choice of the threshold.

The important feature of the damage index (1) is that one can follow its dynamics, associating its increase with the damage development. This allows one to identify if the damage appeared but then stabilized or if keeps progressing.

6   RESULTS

This section presents the analysis for the 32 rpm regime of the wind turbine. Analysis of the 43 rpm and idling regimes is omitted.

The input data is extracted from the database by querying the rotor rpm being in the range [30, 34] and the pitch angle ≤ 0. The query finds 828 samples of the undamaged state, 66 of the 15 cm opening state, 117 samples – 30 cm, 105 – for 45 cm and 500+ for the repaired state. The latter was limited to 500 samples. Signals from accelerometers #5, 8, 9, 11, 12, 14, 15 are used for computing feature vector ($N = 8$, employing dimensionality reduction, with 99.9% variance explained, $K=13$). The model of the normal state is constructed based on the first 400 samples of the normal state; the threshold value is calculated based on the same set, allowing 1% of the samples to be outliers.

Figure 6 illustrates the analysis. The dark green dots represents the normal state; the dots to the left of the vertical dash-dot line are used for training and the threshold value calculation (horizontal dashed line). Four dots (1% of 400) are lying above the threshold, as they are allowed outliers. Model verification is performed using the remaining 428 samples from the normal state. It can be seen that 38 samples of the normal state are located above the threshold; they represent the Type I classification error (false positive or false alarms). They comprise almost 9% of the amount of samples in the verification set, i.e., significantly more than we allowed when forming the normal state modal. This may indicate that the size of the training set is not sufficient to cover all possible operating states, or that the samples are drifting due to some unknown reasons (for example, some slow changes of the SHM's hardware).

The light green crosses represent the samples belonging to the 15 cm crack state. None of the samples is below the threshold, indicating that there are no Type II errors (missed failure).

8

The blue circles and red vertical crosses represent 30 cm and 45 cm crack states, respectively. Both sets are well above the threshold, meaning that 100% of the damage cases are detected. Most importantly, there is clear evidence that the damage index increases with the damage amount, thus we can conclude that the technique is not only capable detecting damage but can also reflects its development.

Finally, the magenta diamonds represent the samples from the repair state. It is clear that for this state, the damage index decreased but did not go below the threshold: indeed, after the repair, the structure still differs from the initial intact state. Thus, a new model of the repaired state is necessary to proceed with monitoring. What is curious is the bursts of the damage index values between samples no. 1300–1400 and around 1500 (denoted by a dashed oval). An ongoing research is supposed to link this observation with either weather conditions or the changes in behaviour of the SHM hardware.
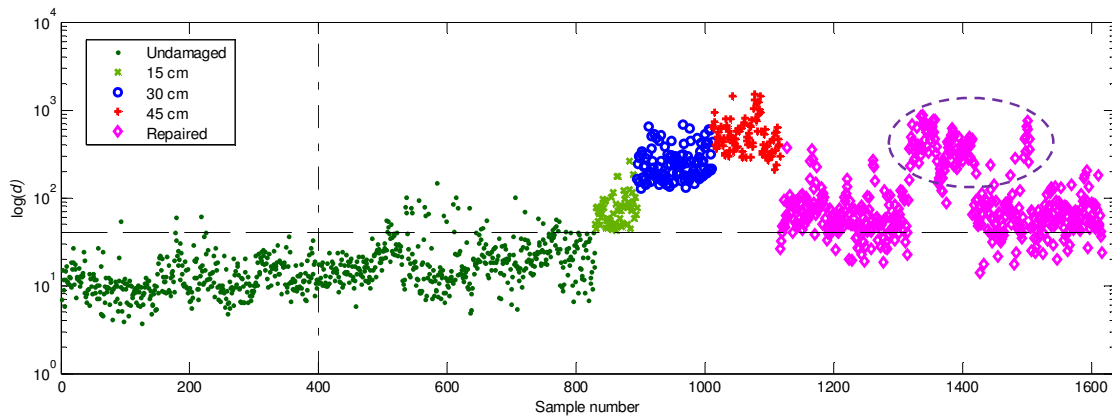

Figure 6. Logarithm of the damage index (1) vs. sample number computed for the 32 rpm wind turbine regime. Left to the dash-dot vertical line: training set; horizontal dashed line: threshold.

7 DISCUSSION

A similar analysis was also performed for two other wind turbine regimes: operating at 43 rpm and idling. While the results of the 43 rpm regime are similar to those presented above, the idling case required taking rotor azimuth angle into account: apparently the samples measured at different blade positions are not directly comparable. A possible reason for this is that while idling, the blade pitch is about 90^0 and the plunger hit direction lies in the rotor plane. Therefore, the strength of the hit is affected by gravity and depends on the azimuth angle (Figure 1c). When operating, the blades' pitch is around zero, the actuator direction is always perpendicular to the vector of gravity (Figure 1b), and the hit strength is not be affected by the rotor position.

8 CONCLUSIONS

The study presents an SHM system that is based on electromechanical actuator (automatic hammer) and an array of accelerometers. As a damage feature, a covariance matrix between the measured acceleration signals was used. The paper describes a three-month long measurement campaign, when the system was installed on operating Vestas V27 wind turbine. The ability of the system to detect an artificially introduced failure (blade's trailing edge opening) was investigated. It was demonstrated that a 15 cm long opening can be detected without stopping the wind turbine. It can be concluded that the actuator-based approach in

9

combination with covariance-based damage feature can be used for successful detection of typical blade defects, while using a feasible hardware setup and semi-supervised learning algorithm.

ACKNOWLEDGMENTS

REFERENCES

[1] C. C. Ciang, J. R. Lee and H. J. Bang, "Structural health monitoring for a wind turbine system: a review of damage detection methods," *Measurement Science and Technology,* vol. 19, no. 21, 2008.

[2] D. T. Griffith, N. C. Yoder, B. Resor, J. White and J. Paquette, "Structural health and prognostics management for the enhancement of offshore wind turbine operations and maintenance strategies," *Wind Energy,* vol. 17, no. 11, pp. 1737-1751, 2013.

[3] M. McGugan, G. Pereira, B. F. Sørensen, H. Toftegaard and K. Branner, "Damage tolerance and structural monitoring for wind turbine blades," *Royal Society of London. Philosophical Transactions A. Mathematical, Physical and Engineering Sciences,* vol. 373, 2015.

[4] G. C. Larsen, P. Berring, D. Tcherniak, P. H. Nielsen and K. Branner, "Effect of damage to modal parameters of a wind turbine blade," in *European Workshop on Structural Health Monitoring*, Nantes, France, 2014.

[5] G. Park, G. T. Taylor, K. M. Farinholt and C. R. Farrar, "SHM of wind turbine blades using piezoelectric active sensors," in *European Workshop on Structural Helath Monitoring*, Sorrento, Italy, 2009.

[6] D. Tcherniak and L. L. Mølgaard, "Vibration-based SHM system: application to wind turbine blades," in *Damage Assessment of Structures*, Ghent, Belgium, 2015.

[7] D. Garcia, D. Tcherniak and I. Trendafilova, "Damage assessment for wind turbine blades based on a multivariate statistical approach," in *International Conference on Damage Assessment of Structures*, Ghent, Belgium, 2015.

[8] M. D. Ulriksen, D. Tcherniak and L. Damkilde, "Damage detection in an operating Vestas V27 wind blade by use of outlier analysis," in *IEEE Workshop on Environmental, Energy and Structural Monitoring Systems (EESMS)*, Trento, Italy, 2015.

[9] M. D. Ulriksen, D. Tcherniak, L. M. Hansen, R. J. Johansen, L. Damkilde and L. Frøyd, "In-situ damage localization for a wind turbine blade through outlier analysis of SDDLV-induced stress resultants," *Structural Health Monitoring,* 2015, submitted.

[10] D. Tcherniak and G. C. Larsen, "Application of OMA to an operating wind turbine: now including vibration data from the blade," in *International Operational Modal Analysis Conference (IOMAC)*, Guimarães, Portugal, 2013.

[11] D. L. Parker, "Multi-objective design optimization framework for structural health monitoring," PhD Thesis, Mississippi State University, 2011.